KSCE Journal of Civil Engineering (2019) 23(4):1670-1681
Copyright ⓒ2019 Korean Society of Civil Engineers
DOI 10.1007/s12205-019-0830-7

Structural Engineering

pISSN 1226-7988, eISSN 1976-3808
www.springer.com/12205

The Effective Width in Shear Design of Wide-shallow Beams: A Comparative Study

Abd El-Hakim Khalil*, Emad Etman, Ahmed Atta***, Ahmed Baraghith****, and Reda Behiry*****

Received April 28, 2018/Revised August 13, 2018/Accepted November 7, 2018/Published Online February 7, 2019

Abstract

In bridges, many architectural constrains lead designers to use wide-shallow beams to support floor loads and transfer forces to columns. An assessment of existing wide-shallow beams in bridges showed that the shear failure is repeatedly governing. This paper provides a comparative study between an experimental research for the shear behavior of wide-shallow beams subjected to static loading and selected on international codes such as the American Association of State Highway and Transportation Officials (AASHTO) practice, the American Concrete Institute (ACI), the Canadian Slandered Association (CSA) and the Euro code (EC2). Seven wide-shallow beams with edge columns were used to investigate the ratios of the beam width to depth (b/d) and the column width to the beam width (c/b) on the performance of shear capacity. The experimental results were presented in terms of deflection, ultimate loads, crack patterns, steel and concrete strains, and shear strain distribution across the width. The results revealed that the shear capacity equations used in the Euro code and the AASHTO are not applicable in wide-shallow beams. An innovated analytical formula to calculate the shear strength of wide-shallow beams is provided in this research.

Keywords: *wide-shallow beams*, *shear strength*, *AASHTO*, *Euro Code, shear design, shear strain*

1. Introduction

Many floor systems contain wide-shallow beams to carry and transfer floor loads to columns. For example, in bridge constructions, a system of wide-shallow beams may provide a simple and economical system to transfer loads from the slab deck to the columns. In many of these design situations, it is advantageous to use diverse beam widths (beams with width wider than the column width) to minimize the reinforcement amount and reduce the overall cost as shown in Fig. 1. The geometric differences in widths between beams and columns will create a difference force flow compared with the traditional narrow beams that support on columns with the same width. Antonio *et al*. (2013) stated that the international codes establish the classification for a "wide-shallow beam", for the purposes of determining the shear capacity, with a beam having a width greater than twice its depth. However, a wide-shallow beam is characterized by some researchers as beams with a depth in general lower than 350 mm and a cross section where the width (b) over the effective depth (d) ratio is greater than 2 (i.e., $b/d > 2$); even though the common values of effective depth (d) are 250–300 mm and b/d are 4–5.

Recently, some researchers focused on the shear behavior of wide-shallow beams. Lubell *et al*. (2009a) and Serna *et al.* (2002) investigated the relationship between the stirrups cross spacing and the shear strength of wide-shallow beams. The research concluded that the effectiveness of stirrups increases as the transverse spacing between the web reinforcement decreases. Also, the mode of failure is more ductile when the spacing between stirrups legs is less than a distance of twice the member height. Sherwood *et al.* (2007) carried out a comparative study between wide-shallow beams and thick slabs in shear behaviour. They concluded that the cracking shear stresses of slabs and wide-shallow beams are approximately similar.

The influence of the member width on the shear behavior was studied also by Antonio *et al.* (2015). The test series compared the capacities of wide and narrow specimens having the same depth and the same longitudinal reinforcement amount. They obtained shear stresses at failure for the wide specimens that didn't vary by more than 10% from the companion narrow specimens. Thus, they concluded that the member width was a significant parameter in predicting the shear capacity at failure.

*Professor, Dept. of Structural Engineering, Tanta University, Tanta 31511, Egypt (E-mail: a370160@yahoo.com)
**Professor, Dept. of Structural Engineering, Tanta University, Tanta 31511, Egypt (E-mail: emad.etman@f-eng.tanta.edu.eg)
***Professor, Dept. of Structural Engineering, Tanta University, Tanta 31511, Egypt (Corresponding author E-mail: Drahmedatta2003@yahoo.com)
****Assistant Professor, Dept. of Structural Engineering, Tanta University, Tanta 31511, Egypt (E-mail: ahmed_baraghit@yahoo.com)
*****Assistant Professor, Dept. of Structural Engineering, Tanta University, Tanta 31511, Egypt (E-mail: Redabehiry@yahoo.com)



Fig. 1. Wide-shallow Beams Application in RC Bridges

Also, Antonio *et al.* (2017) evaluated the influence of both the *b*/*d* and bar spacing-to-effective depth ratio (*s*/*d*) on the shear strength of reinforced concrete elements without the web reinforcement by means of an experimental program on full-scale specimens characterized by *b*/*d* ranging from 0.5 to 3.5 and an *s*/*d* from 0.24 to 0.71. Results showed that for *b*/*d* > 1, an increase in b/d determines a non-negligible increment in the shear strength, whereas *s*/*d* (in the considered range) does not affect the shear bearing capacity.

The influence of the longitudinal reinforcement ratio on the shear capacity was investigated by Lubell *et al.* (2009b). They tested six specimens with varying the depth and longitudinal reinforcement ratio. The depth of the tested specimens ranged from 287 to 538 mm and the flexure reinforcement ratio varied from 0.33 to 1.73%. It demonstrated that the ratio of flexural reinforcement increased the shear load. Mohammadyan *et al.* (2014) carried out a comparative study on the shear capacity of six reinforced concrete wide-shallow beams with diverse types of reinforcement. The results concluded that using bent-up bars in shear reinforcement has a significant improvement on the shear strength of wide-shallow beams. The combination of bent-up bars with stirrups led to a higher shear capacity and gradual failure of the specimens.

2. Codes' Review for Shear of Wide-shallow Beams

2.1 American Concrete Institute ACI (2008)

The nominal shear capacity (V_n) that is calculated according to ACI (2008) is the sum of the concrete contribution (V_c) and the web reinforcement contribution (V_s), which is calculated by the following equations:

$$V_n = V_c + V_s \tag{1}$$

$$V_c = 0.17\lambda\sqrt{f'_c}b_w d \tag{2}$$

$$V_s = \phi f_{yt}\, d\, \frac{A_v}{s} \tag{3}$$

2.2 Euro Code 2-2004 (EN 1992-1-1, 2004)

According to EC2-2004: The shear resistance of concrete ($V_{Rd,c}$) can be estimated by the following equations:

$$V_{Rd,c} = [C_{Rd,c}k(100\rho f_{ck})^{1/3}]b_w d \tag{4}$$

$$k = 1 + \sqrt{\frac{200}{d}} \le 2.0 \tag{5}$$

$$C_{Rd,c} = 0.18/\gamma_c \tag{6}$$

For beams with web reinforcement, the shear resistance by the web reinforcement, $V_{Rd,s}$, is given by the following equation:

$$V_{Rd,s} = \frac{A_{sw}}{s_v} z f_{yw} \cot\theta \tag{7}$$

2.3 AASHTO LRFD Bridge Design Specifications (AASHTO, 2005)

The Modified Compression Field Theory (MCFT) that is used in AASHTO Load Resistance Factor Design (LRFD) section design model for shear is based on the nominal shear resistance (V_n), which is the sum of the concrete contribution (V_c) and the web reinforcement contribution (V_s) and computed by the following equations:

$$V_n = V_c + V_s \tag{8}$$

$$V_c = 0.083\beta\sqrt{f'_c}b_v d_v \tag{9}$$

$$V_s = \frac{A_v}{s_v} d_v f_{yv}(\cot\theta + \cot\alpha)\sin\alpha \tag{10}$$

2.4 Canadian Standards Association (CSA, 2004)

The CSA specifications calculate the shear capacity for reinforced concrete members with the web reinforcement, as shown in the following equations:

$$V_u = V_c + V_s \tag{11}$$

$$V_c = \phi_c\lambda\beta\sqrt{f'_c}b_w d_v \tag{12}$$

$$V_s = \frac{\phi_s A_v f_{yt} d_v}{\tan\theta\, s_v} \tag{13}$$

3. Research Significance

This paper investigates the effect of the following parameters on the shear behavior of wide-shallow beams: 1) beam width to depth ratio (*b*/*d*) and 2) columns' width to beam width ratio (*c*/*b*). Moreover, the research assesses the adequacy of international codes formulas in the shear capacity of wide-shallow beams. At the end of this research, an innovated analytical formula is obtained to calculate the shear strength of reinforced concrete wide-shallow beams.

4. Experimental Program

The experimental work for the shear behavior of reinforced concrete wide-shallow beams is presented. The specimens consisted of identical concrete mixtures and configurations, including a beam part and a column part to support the real condition of beam- columns.

4.1 Specimen's Description

Seven reinforced concrete specimens were tested under a four point static loading system. The shear span to depth ratio (*a*/*d*) of 2.25 was chosen achieve shear failure for all specimens. This value was chosen according to previous researches related to wide-shallow beams (Lantsoght *et al.,* 2014; Sherwood *et al..* 2006). The total height of all beams is 250 mm and the gross cover is 50 mm, corresponding to an effective depth of 200 mm. The geometry of the specimens and the reinforcement details are presented in Fig. 2 and summarized in Table 1. Moreover, the minimum amount of the web reinforcement according to ACI (2008) was also produced for all tested beams. Stirrups with four-legs having a diameter of 8 mm at a constant longitudinal spacing of 200 mm was used. A constant area of longitudinal reinforcement was placed; in particular, seven rebar's having a diameter of 22 mm were disposed as a main reinforcement to prevent flexure failure and seven rebar's with a diameter of 12 mm were used in the top to fix the stirrups in position. It is worth mentioning that the longitudinal reinforcement ratio is an important parameter affecting the shear strength of Reinforced Concrete (RC) beams, especially in narrow beams. But in wide-shallow beams, this effect is insignificant as it affected on the results by a value around 2% only, as calculated according to the ACI (2008) equations which can be neglected in analysis. It should be noticed that the column parts were reinforced properly with stirrups and axial reinforcement using an appropriate anchorage length of the bars in order to resist the applied load at failure.

The experimental program was divided into two groups: 1)

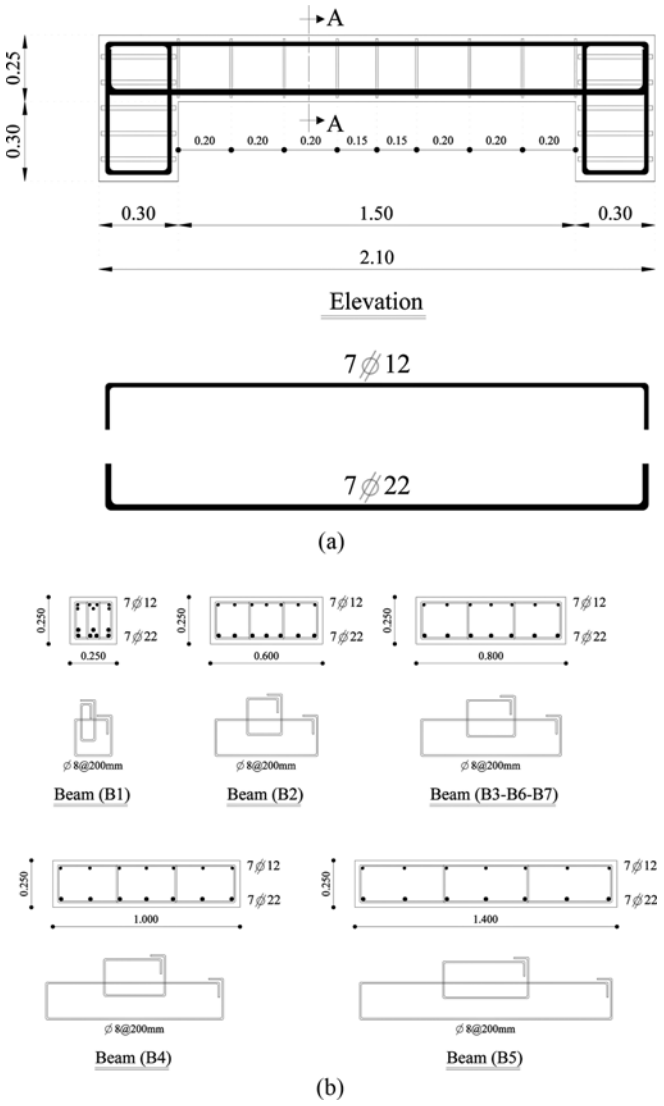


Fig. 2. The Geometry of the Specimens and the Reinforcement Details: (a) Elevation of Tested Specimens, (b) Section A-A for All Specimens

Table 1. Main Characteristics of Test Specimens

Group (I)								
Specimen	*b* mm	*d* mm	*c* mm	*b*/*d*	*c*/*b*	Tension R.F.T	Compression R.F.T	Shear R.F.T
B1	250	200	250	1.25	1.00	7Ø22	7Ø12	Ø8@200mm
B2	600	200	600	3.00	1.00	7Ø22	7Ø12	Ø8@200mm
B3	800	200	800	4.00	1.00	7Ø22	7Ø12	Ø8@200mm
B4	1,000	200	1,000	5.00	1.00	7Ø22	7Ø12	Ø8@200mm
B5	1,400	200	1,400	7.00	1.00	7Ø22	7Ø12	Ø8@200mm
Group (II)								
Specimen	*b* mm	*d* mm	*c* mm	*b*/*d*	*c*/*b*	Tension R.F.T	Compression R.F.T	Shear R.F.T
B6	800	200	200	4.00	0.25	7Ø22	7Ø12	Ø8@200mm
B7	800	200	400	4.00	0.50	7Ø22	7Ø12	Ø8@200mm
B3	800	200	800	4.00	1.00	7Ø22	7Ø12	Ø8@200mm

Note: *b* = width of beam section, *d* = effective depth of beam section, *c* = width of column section, perpendicular length to centerline of beam.

group I consisted of five specimens varied in width to a depth ratio (b/d) from 1.25 to seven; and 2) group II which consisted of three specimens with a constant b/d of 4.00 and a different column width to beam width ratio (c/b) ranging from 0.25 to 1.00.

4.2 Material Properties

Ready mixed concrete containing coarse aggregate of 20 mm maximum size and a nominal specified strength of 30 MPa was used. Seven standard cylindrical molds, one cylinder for each specimen, were casted at the same time as the specimens and cured for control tests. Concrete samples were tested according to ASTM (2014a) and ASTM (2014b); the results are presented in Table 2. Reinforcement rebars of 8, 12, and 22 mm were used for stirrups, compression reinforcement, and tension reinforcement, respectively. The actual yield and ultimate stress for the used bars of different diameters were evaluated according to ASTM (2016), as shown in Table 3.

Table 2 Concrete Characteristics

Cylinder	Diameter mm	Height mm	P_{max} kN	f_c MPa	E_c MPa	υ
B1	150	300	485	27.40	25,052	0.247
B2	151	302	482	26.91	24,880	0.218
B3	151	300	497	27.70	25,608	0.223
B4	150	300	517	29.26	24,234	0.235
B5	150	300	538	30.40	27,863	0.249
B6	151	301	522	29.15	27,753	0.244
B7	150	300	485	27.30	25,098	0.242

Note: P_{max}= maximum testing load, f_c = compressive stress, E_c = static modulus of elasticity, υ = Poisson's ratio of concrete.

Table 3. Reinforcement Characteristics

Bar No.	Area mm^2	f_y MPa	f_u MPa	ε_y μs
D8	50.30	355	484	1,200
D12	113	446	637	2,200
D22	380	406	624	2,150

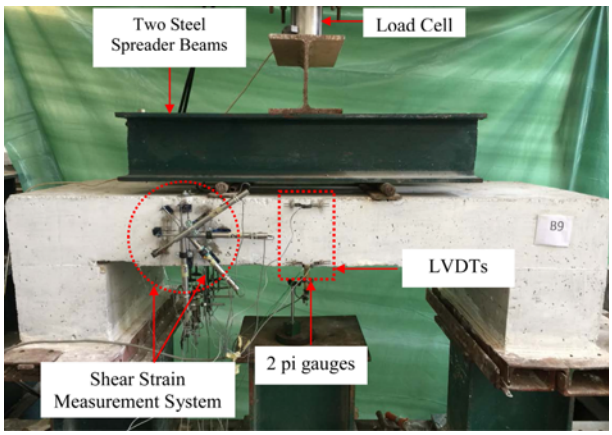


Fig. 3. Laboratory Photo Instrumentation and Test Setup

4.3 Test Set-up and Instrumentation

All tested beams were loaded symmetrically with two equal fully width line loads, as shown in Fig. 3, which resulted in a region of a nearly constant moment over the central part of the beam. Instrumentations for all specimens were designed to capture the load-deformation behavior, and determine variations in reinforcement strains, and concrete strains along the tested

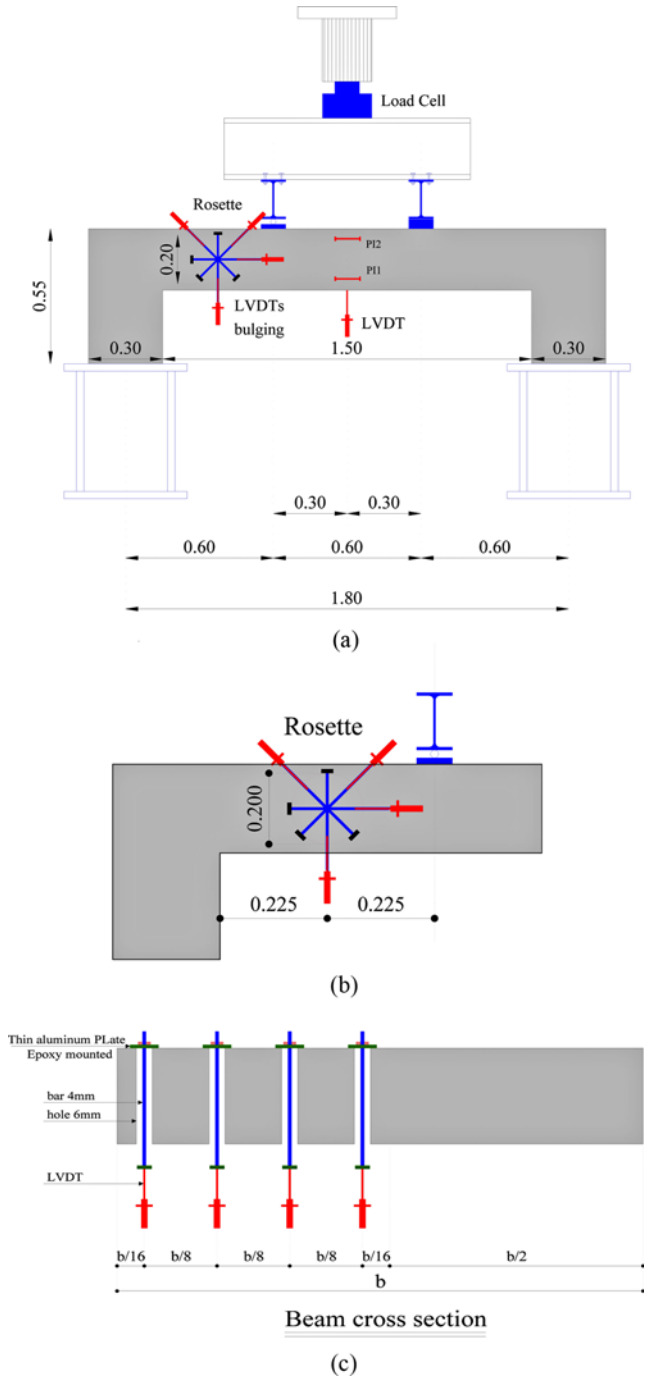


Fig. 4. Schematic Instrumentation and Test Setup: (a) Sketch for Dimension of Test Setup, (b) The System of LVDTs to Obtain Shear Stress, (c) The System of LVDTs-based Bulging Gauges

beam widths. The used load cell was calibrated prior to use. A manual hydraulic jack with a maximum capacity of 1,200 kN loaded the beams by applying a downward load by an increment of 1.0 kN up to failure and was measured by the load cell attached to the jack. Vertical displacement measurements were recorded from the Linear Variable Differential Transformers (LVDTs) to capture differential deformations across the width of the members. The test setup for loaded specimens is depicted in Fig. 4(a).

On the side faces, the shear strains were measured using one circular rosette of four LVDTs, as shown in Fig. 4(b). A system of LVDTs-based bulging gauges was used to measure the shear strain distibution across the beam width by measuring the vertical increase of the member thickness caused by diagonal cracking, as shown in Fig. 4(c). The holes through the concrete for the bulging gague were formed with a 6 mm diameter flexiable plastic tubing that was removed prior to the tests. The free movment of the LVDTs piston prevented the gague from action as a force-resisting element. Electrical strain gauges were mounted on the longitudinal bars at mid-span and for each stirrup leg in the shear span. One electrical pi-gagues, 100 mm in length, was mounted on the top surface of the specimen at mid-spanto to determine the concrete flexure strain at the compression zone.

5. Experimental Results and Discussions

5.1 Crack Patterns and Failure Modes

In the early stages of loading, the beams were free of cracks. When a maximum tensile stress in the concrete was reached,

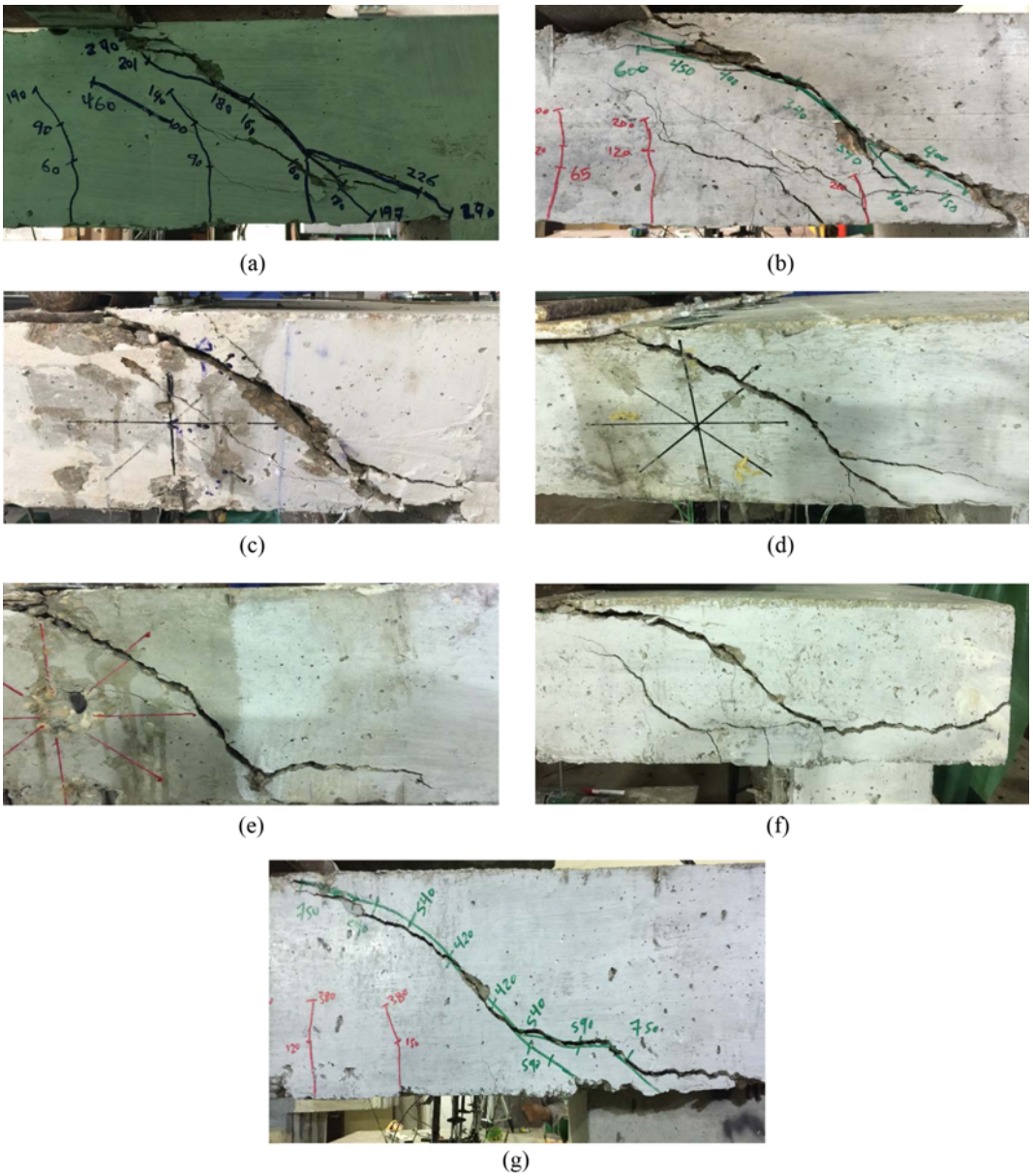


Fig. 5. Final Crack Pattern of Tested Specimens: (a) Specimen B1, (b) Specimen B2, (c) Specimen B3, (d) Specimen B4, (e) Specimen B5, (f) Specimen B6, (g) Specimen B7

vertical flexural cracks formed from the tension zone of the beam at intervals along the constant moment region. After the flexural cracks had extended upward a short distance above the longitudinal reinforcement, they extended further vertically in the pure moment zone. After the flexural crack had formed, a small diagonal crack appeared suddenly slightly above the main steel level and at approximately the middle of the shear span. As the load increased, the inclined shear crack developed further towards the loading points and the supports. The rate of propagation of the inclined shear crack was different as *b*/*d* changed. Correspondingly, the ultimate failure of the tested beams took different forms with a variation of the width to depth ratio (*b*/*d*). In group I, a narrow beam (B1) where the *b*/*d* ratio equals 1.25, the inclined shear crack propagated very gradually toward the load point and eventually crushing occurred somewhat above the crack in the reduced section. When the inclined shear crack reached a point somewhere above the neutral axis, several local diagonal cracks were formed at the level of the tension reinforcement and gradually connected with each other. For this beam, the formation of the inclined shear crack did not cause failure; the substantial additional load was resisted after the inclined shear crack was initiated. The failure was sudden and loud and this failure mode is conventionally called a shear compression failure, as shown in Fig. 5(a).

For the wider specimen (B5) where the *b*/*d* ratio equals 7.00, the inclined shear crack propagated suddenly and extended directly to the top surface of the beam with little change in load. A very thin concrete segment was left above the inclined shear crack without any evidence of crushing. This failure mode is conventionally called a diagonal tension failure, as shown in Fig. 5(e). For wide-shallow beams (B2, B3, and B4) with *b*/*d* ratios of 3.00, 4.00, and 5.00, the crack pattern fell between the two cases mentioned above, as shown in Figs. 5(b), 5(c), and 5(d). This indicates that the failure modes are directly related to the stability of the inclined shear cracks, which depends on the b/d ratio. The inclined shear crack in beam B2 can be classified as an unstable crack because it propagated quickly without any additional load, resulting in the separation of the member into two pieces. Whereas in beams B3 and B4, an additional load was needed to extend the inclined shear crack so that these cracks may be identified as stable cracks.

In group II, the flexural cracks began during the first loading stages. Then, the diagonal cracks appeared as the applied load increased. At the final stages of loading before failure ($P > 0.85 P_{max}$), the diagonal cracks rapidly widened and extended upwards to the loading point. For specimens B3, in which the support width extended to the specimen edge, the shear cracks terminated at the edge of the supporting columns, as shown in Fig. 4(c). However, when a narrow support was used, the shear crack extended horizontally and past the centerline of the specimen, as shown in Figs. 5(f) and 5(g). The difference in the crack extent is explained by the lack of confining pressure in the latter case, which allows tensile splitting cracks to form.

5.2 Cracking and Ultimate Loads

Table 4 summarizes the results of tested specimens, which include the first flexural and shear cracking loads, the maximum ultimate load and the maximum deflection. The flexural and diagonal cracking loads were determined from the direct observation of the crack patterns during the test. The stirrup strain measurements were also used to determine the diagonal cracking load as the load at which first a significant increase of the stirrup strain crossing the inclined crack occurred.

In group I, it is clear that the relationship isn't linear between the ultimate load and the width of the beam, i.e., doubling the width of a beam wouldn't point to doubling the shear strength (keeping all the various variables affecting the shear response constant). Increasing the *b*/*d* from 1.25 to 5.00 (four times), leads to an increase of about 132% in the ultimate shear strength. In group II, specimen B3 ($c/b = 100\%$) has the higher diagonal cracking load and the higher ultimate load. It is clear that the diagonal cracking load was insignificantly increased with the increase of the *c*/*b* ratio. By increasing the column width to the beam width ratio (*c*/*b*) from 25% to 100%, the ultimate load

Table 4 Specimen Properties and Test Results

Group (I)									
Specimen	*b* mm	*d* mm	*c* mm	*b*/*d*	*c*/*b*	Flexural cracking load (kN)	Shear cracking load (kN)	Ultimate load (kN)	Max. deflection (mm)
B1	250	200	250	1.25	1.00	35	171	397	11.62
B2	600	200	600	3.00	1.00	73	407	735	12.20
B3	800	200	800	4.00	1.00	95	540	809	9.45
B4	1,000	200	1,000	5.00	1.00	116	648	884	7.71
B5	1,400	200	1,400	7.00	1.00	160	869	1,035	10.72
Group (II)									
Specimen	*b* mm	*d* mm	*c* mm	*b*/*d*	*c*/*b*	Flexural cracking load (kN)	Shear cracking load (kN)	Ultimate load (kN)	Max. deflection (mm)
B6	800	200	200	4.00	0.25	75	528	655	17.99
B7	800	200	400	4.00	0.50	80	537	736	13.73
B3	800	200	800	4.00	1.00	95	540	809	9.45

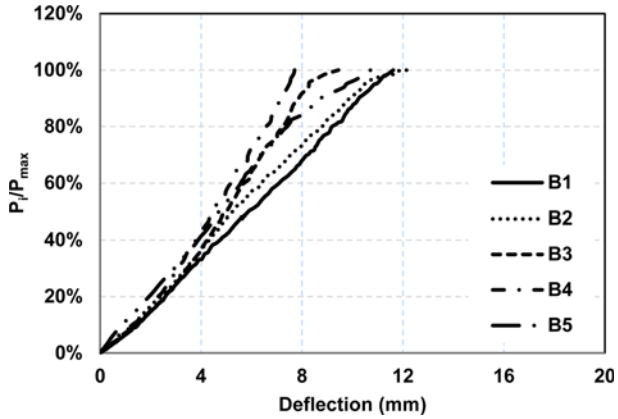


Fig. 6. Experimental Curves of the Normalized Load (P_i/P_{max}) vs. Mid-span Deflection for Group (I)

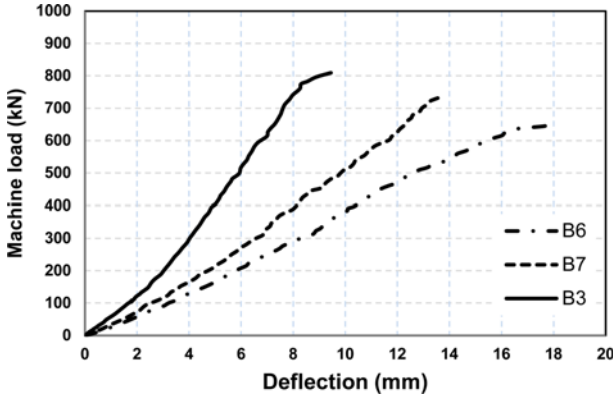


Fig. 7. Experimental Curves of the Machine Load vs. Mid-span Deflection for Group (II)

increased by about 24%. Also, the ultimate load was increased by about 10% as *c*/*b* increased from 50% to 100%.

5.3 Load-deflection Relationships

Figure 6 shows the deflection verse load for the tested beams of group I at mid-span. As presented in this figure, the general trend of the load-deflection curves was similar among the tested beams despite the change of the beam width to depth ratio (*b*/*d*). The load-deflection curves of specimens may be roughly described by a bilinear relationship. The first stage starts from the beginning of the loading up to the point at which an inclined shear crack was first observed. In this stage, the beams acted linearly and the slopes (stiffness) were dependent on *b*/*d* ratio. As expected, at the same load level, the mid span deflection increased as *b*/*d* decreased due to the decrease of the cross section inertia of the tested beam. The second stage starts from the point of the inclined shear crack initiation to the point of the ultimate load. Around the inclined shear cracking load, the stiffness generally started to decrease more rapidly. For the narrow beam (B1) where *b*/*d* ratio equals 1.25, the stiffness decreased. However, for other specimens, the stiffness considerably changed just after the inclined shear cracks were initiated. It was noted, that the vertical axis indicates the machine load over the ultimate maximum load to normalize the results for different widths.

In contrast to the typical behavior of wide-shallow beams with full supporting in flexure, the load-deflection relationship of specimens in group II did not exhibit a sudden change of the slope in the load-deflection plot at the first stage of loading, as shown in Fig. 7. By increasing the load, the relationship for all specimens took a non-linear trend at the end of the testing with a gradually reducing slope. After some additional deformation, a significant diagonal crack formed leading to a shear failure, then a sudden and large drop in the load was recorded at failure.

5.4 Strains

5.4.1 Concrete and Main Reinforcement

Figures 8 and 9 show the load versus main reinforcement tensile strain in the right side and the compression strain of concrete in the left side. It was noticed that the recorded main steel strains did not reach the yielding strains (2,150 μs) and also the compression strain did not reach the value of the maximum compression strain in flexure (3,500 μs) according to ACI (2008). This ensured that the modes of failure of these specimens were governed by shear not by flexural failure.

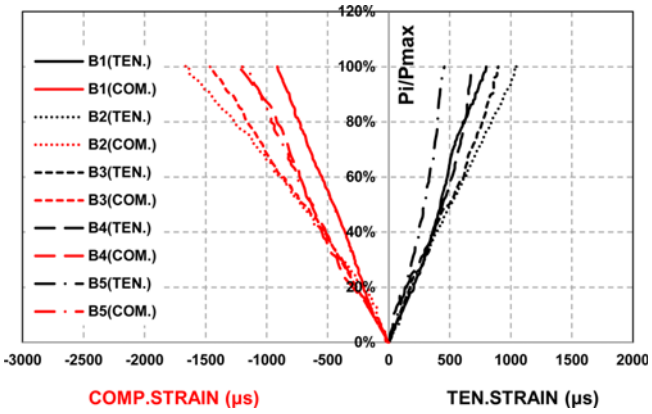


Fig. 8. Experimental Curves of the Normalized Load (P_i/P_{max}) vs. Flexure Strain in Concrete and RFT for Group (I)

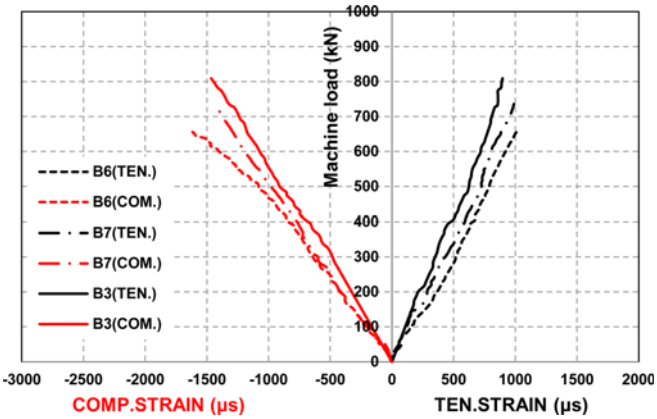


Fig. 9. Experimental Curves of the Machine Load vs. Flexure Strain in Concrete and RFT for Group (II)

5.4.2 Stirrup Strains

Figures 10 and 11 show the shear stress ($P_i/(b.d)$) versus tensile strain of the outer stirrup leg in the right side and the tension strain of the inner stirrup leg in the left side for groups I and II, respectively. In all specimens, the first part of the relationship is defined by a line starting at the origin and extending along the vertical axis up to the appearance of the first inclined shear cracking. This behavior indicates that, initially, the stirrups did not contribute to the shear capacity of the beam until an inclined crack developed. However, after inclined cracking, the second region of the shear stress-strain relationship started and extended up to the failure of all specimens.

For the narrow beam (B1), it appears that the tensile strain in the inner and outer stirrup legs is the same at any load level and equal to 800 micro strains at ultimate. This assures that the shear stress distribution along the width of the narrow beam B1 is constant. However, for other wide-shallow beams, the average tensile strain in the inner stirrup legs is about 33% of the average tensile strain in the outer stirrups which indicates that the shear strain distribution on the width of these beams is variable. For specimen B6 with a supporting column width equal to 25% of the beam width, the inner stirrups tensile strain reached to yield strain (1,209 micro strains), however the tensile strain of the outer stirrups is 460 micro strains, 38% of the yield strain which points out the generating of a column strip between the supporting columns. On the other hand, the behavior of strains for specimen B3 (full width supporting specimen) is in the opposite way, the inner stirrups tensile strain reached 417 micro strains (35% of the yield strain), however the tensile strain of the outer stirrups reached the yield strain.

5.4.3 Strain Distribution along the Width

Figure 12 shows the strain distribution along the tested beams' width of group I that was measured using a system of LVDTs-based bulging gauges. By analyzing the curve of the narrow beam (B1), it is evident that the shear strain is approximately constant over the cross section. However, the shear strains for wide-shallow beams have the minimum values at mid-point and the maximum values at the outer point. For the wide-shallow beams (B2, B3, B4 and B5), the shear strain at mid-point decreased by an average of 27%, compared with the value at the outer face. This conclusion leads to that the width of the cross section is a very important parameter in the design implication for shear in wide-shallow beams. However, the changing of the

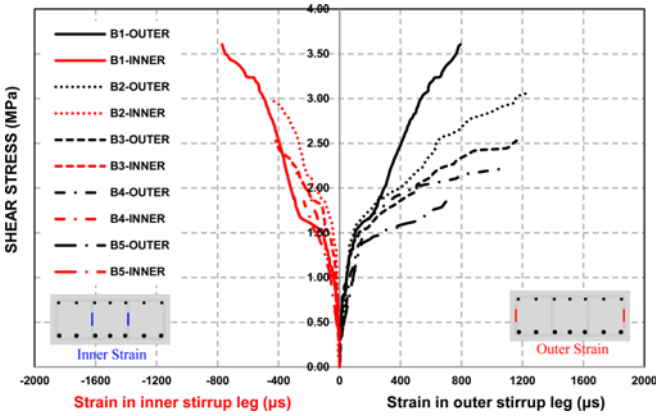


Fig. 10. Shear Stress vs. Tensile Strain in Outer and Inner Stirrups for Group (I)

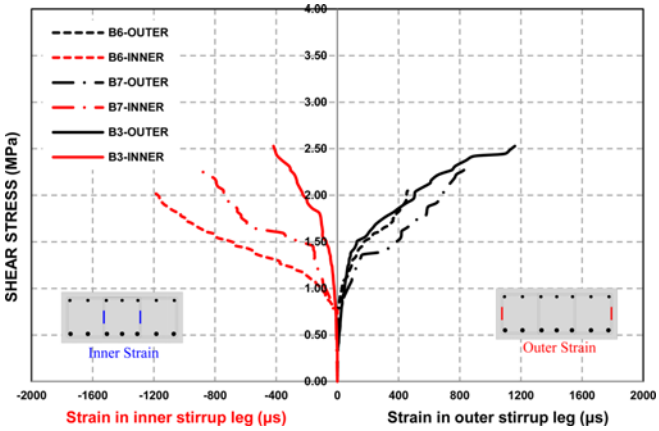


Fig. 11. Shear Stress vs. Tensile Strain in Outer and Inner Stirrups for Group (II)

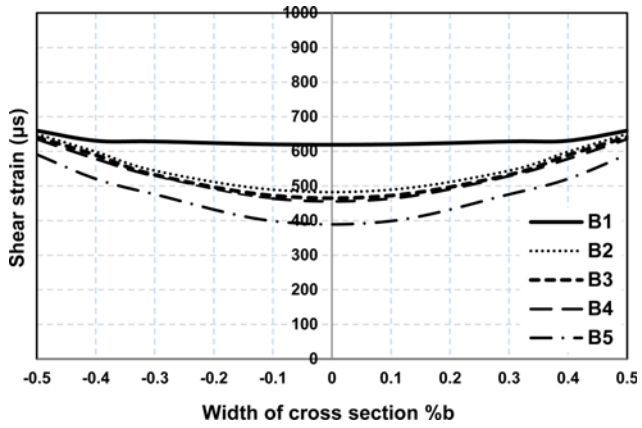


Fig. 12. Shear Strain Distribution along the Width of Specimens in Group (I)

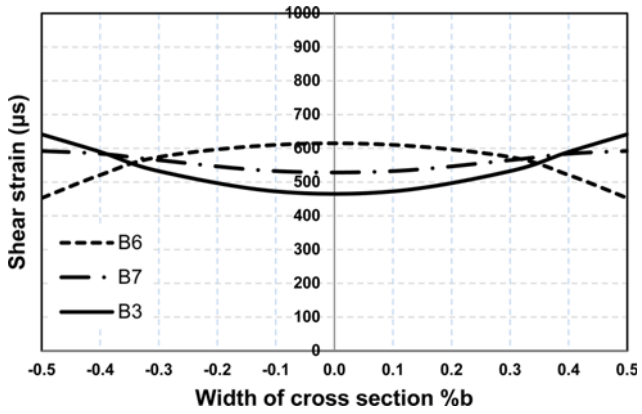


Fig. 13. Shear Strain Distribution along the Width of Specimens in Group (II)

column width to beam width (c/b) from 25% to 100% has a strong prominence on the shear-strain distribution along the width of reinforced concrete wide-shallow beams, as shown in Fig. 13. The shear-strain distribution trend of the narrow column is in contrast to the trend of the wide column. The maximum strain was at mid-width for the narrow column but was at the face of the width for the wide columns.

6. Comparing Codes and Previous Studies

Table 5 shows a number of predictive shear design formulas for beams in different design codes and technical literature. The comparison between the experimental shear cracking load (V_{exp}) and the shear strength predicted by code formulas (V_{pre}) is presented in Fig. 14. It can be observed that ACI (2008) and AASHTO (2005) codes are conservative; however the estimations that were obtained by using EN 1992-1-1 (2004) and CSA (2004) are un-conservative in some cases. The underestimation by codes was expected because all codes mainly consider the shear strength of reinforced concrete beams equal to the inclined first cracking shear and this conclusion confirms that the contribution of concrete formals of the international codes must be recalibrated. Also, it is obvious that the other equations obtained from the technical literatures couldn't exactly predict the shear strength of wide-shallow beams. So, a design equation for calculating the shear strength of wide-shallow beams is required.

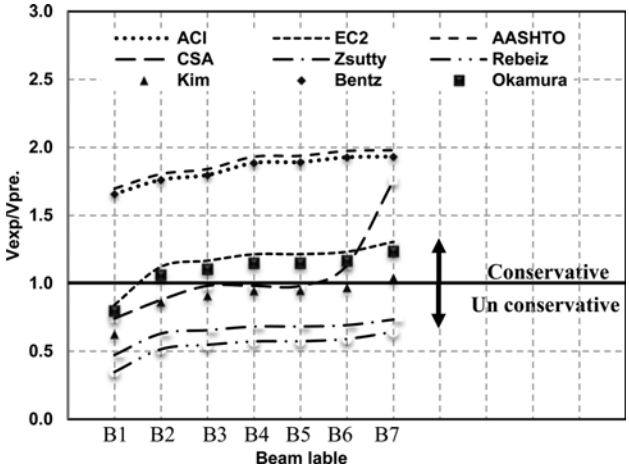


Fig. 14. Experimental vs. Predicted Shear Force

7. Proposed Design Recommendations

One of the significant differences between narrow beams and wide-shallow beams is the ratio of beam width to depth (b/d). The different codes and technical literatures didn't take the effect b/d and c/b into consideration which leads to a major error in

Table 5 Predictive Equations for Shear Strength of RC Beams

Reference	Predictive equation
ACI 318-08 (2008)	$V_c = 0.17\lambda\sqrt{f'_c}bd$
EC2-04 (2004)	$V_{Rd,c} = \lfloor C_{Rd,c}k(100\rho f_{ck})^{1/3} \rfloor bd$
AASHTO LRFD-05 (2005)	$V_c = 0.083\beta\sqrt{f'_c}bd$
CSA A23.3-04 (2004)	$V_c = \phi_c\lambda\beta\sqrt{f'_c}bd$
Zsutty (1968)	$V_c = 2.20\left(f'_c\,\rho\frac{a}{b}\right)^{1/3}\left(\frac{2.5d}{a}\right)bd$
Rebeiz (1999)	$V_c = \left(0.40 + 2.50\sqrt{f'_c\,\rho\frac{a}{b}}\right)bd$
Kim and Park (1996)	$V_c = \left\{3.50(f'_c)^{1/3}\rho^{3/8}\left(0.40+\frac{d}{a}\right)\left(\frac{1}{\sqrt{1+.0008d}}+0.18\right)\right\}bd$
Bentz (2005)	$V_c = \frac{200}{1000+31.5\frac{d}{a_g+16}}\sqrt{f'_c}bd$
Okamura and Higai (1980)	$V_c = 0.20\frac{(100f'_c\,\rho)^{1/3}}{\left(\frac{d}{1000}\right)^{1/4}}\left(0.75+\frac{1.40}{a/d}\right)bd$

computing the shear strength of wide-shallow beams. In the present study, it was of interest to understand whether wider members would have higher shear capacities than similar narrow beams. Also, it was important to determine whether the beam width to depth ratio (b/d) and the column width to beam width ratio (c/b) are significant parameters in predicting the shear capacity of wide-shallow beams. Thus, a laboratory testing was conducted to directly evaluating the influence of b/d and c/b on the shear capacity of such beams. The investigation of the analysis of the parameters b/d and c/b showed that the aforementioned parameters are significant in predicting the shear capacity of wide-shallow beams. This was determined using the test data of beams tested in this research having width to depth ratios of 1.25, 3.00, 4.00, 5.00, and 7.00 and column width to beam width ratios equal to 25%, 50%, and100%. Recalling the data from the relationships between the b/d ratio and the shear strain distribution across the width of the member, the shear stress distribution for the narrow beam is constant but the relationship took a non-linear shape for wider-shallow beams. The effective width (b_{eff}) for each specimen was calculated by the following equations based on statistical procedure:

$$b_{eff} = 0.47 \times b \frac{(c/b)^{0.18}}{(b/d)^{0.10}} \quad (14)$$

The nominal shear capacity can be calculated by the following:

$$V_n = V_c + V_s \quad (15)$$

$$V_c = b_{eff} \cdot d \sqrt{f_c'} \quad (16)$$

$$V_s = A_{st} \cdot f_{yst} \frac{d}{S_L} \quad (17)$$

8. Validation of the Proposed Analytical Model

Wide-shallow beams tested in the current research were assembled to be used for the validation of the proposed analytical model. Fig. 15 presents the comparison between the predicted shear capacities that were calculated by the proposed analytical model and the experimental shear capacities obtained from the tested specimens in the current study. The analytical shear model gives satisfied predictions for the shear capacity of wide-shallow beams.

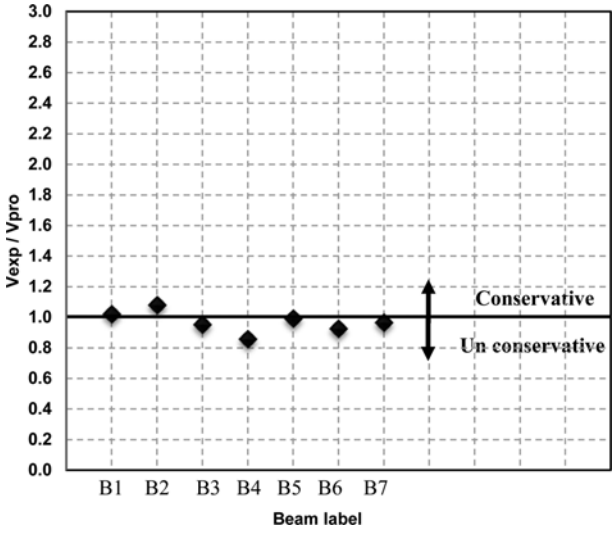


Fig. 15. Validation of the Proposed Analytical Model with the Experimental Results.

9. Conclusions

The behavior of reinforced concrete wide-shallow beams was analyzed in this paper by focusing on the effect of the beam width to the depth ratio (b/d) and the column width to the beam width ratio (c/b). Based on the experimental and analytical results obtained in this study, the subsequent conclusions can be listed as follow:

1. There was a substantial difference in the performance of shear-critical narrow beams, and wide-shallow beams on a unit width basis, for members with uniform construction across the width.
2. The beam width to depth (b/d) ratio has a significant influence on the modes of failure and the shear strength for reinforced concrete wide-shallow beams.
3. The use of support narrower than the member width decreased the one way shear strength of beams relative to the full-width condition.
4. For a wide-shallow beam, simply-supported on a narrow column, the distribution of shear strains varies across the beam width. Furthermore, this distribution changes from that of typically higher strains in the outer face to higher strains in the middle in case of full support along the width.
5. Most of previous analytical models that used to estimate the shear strength of reinforced concrete wide-shallow beams disregarded the losses in shear resistance due to the different values of the width to depth ratio (b/d) and the support width to the beam width ratio (c/b).
6. Capacity modification factors were developed to reduce the concrete shear capacity of reinforced concrete wide-shallow beams to account for the influence of the beam width to the depth ratio (b/d) and the columns width to the beam width ratio (c/b).
7. The study proposed a modified formula that clearly showed a great improvement in predicting the effective width (b_{eff}) that is used in shear capacity.

Notations

A_v = The area of shear reinforcement according to ACI 318-08, AASHTO-05, and CSA A23.3-04 (mm^2)
A_{sw} = The area of shear reinforcement according to EC2-2004
b = The web width of section according (mm)
d = The distance from the extreme compression fiber to the central axis of the longitudinal reinforcement according to

ACI 318-08 and EC2-2004 (mm)

b_v = The web width of section according to AASHTO-05 (mm)

d_v = The distance from the extreme compression fiber to the central axis of the longitudinal reinforcement according to CSA A23.3-04 and AASHTO-05 (mm)

b_w = The web width of section according to ACI 318-08, EC2-2004, and CSA A23.3-04 (mm)

f_c' = The concrete compressive cylinder strength (MPa).

f_{ck} = The characteristic concrete cube strength (MPa).

f_{yst} = The yield strength of the transverse reinforcement according (MPa)

f_{yt} = The yield strength of the transverse reinforcement according to ACI 318-08 and CSA A23.3-04 (MPa).

f_{yv} = The yield strength of the transverse reinforcement according to AASHTO-05 (MPa)

f_{yw} = The yield strength of the transverse reinforcement according to EC2-2004 (MPa)

V_c = The nominal shear strength provided by concrete.

V_n = The nominal shear strength (N)

V_u = The factored shear force at the section (N)

$V_{Rd,c}$ = The nominal shear strength provided by concrete according to EC2-2004

V_s = The nominal shear strength provided by shear reinforcement (N)

$V_{Rd,s}$ = The nominal shear strength provided by shear reinforcement according to EC2-2004 (N)

S = The spacing of the transverse reinforcement according to ACI 318-08 (mm)

S_v = The spacing of the transverse reinforcement according to EC2-2004, AASHTO-05 and CSA A23.3-04 (mm)

S_l = The spacing of the transverse reinforcement (mm)

z = The inner lever arm for a member with constant depth according to EC2-2004 (mm)

θ = The angle between inclined concrete struts and the main tension chord

α = The angle of inclined stirrups to longitudinal axis

β = The factor indicating the ability of diagonally cracked concrete to transmit tension according to AASHTO-05

λ = The strength reduction factor for concrete according to ACI 318-08

$\emptyset$ = The strength reduction factor for reinforcement according to ACI 318-08

$\emptyset_s$ = The resistance factor for reinforcement according to CSA A23.3-04

$\emptyset_c$ = The resistance factor for concrete according to CSA A23.3-04

ρ = The tensile reinforcement ratio according to EC2-2004

γ_c = The concrete partial safety factor according to EC2-2004

Acknowledgements

The authors appreciate the technical staff of the Reinforced Concrete and Heavy Structures Laboratory, Faculty of Engineering, Tanta University, Egypt. Also, this study is a part of the Ph.D. thesis in shear behavior of wide-shallow beams.

References

AASHTO (2005). *Bridge design specifications and commentary*, 3rd Edition, American Association of State and Highway Transportation Officials.

ACI (2008). *Building code requirements for structural concrete (ACI 318-08) and commentary*, American Concrete Institute, Farmington Hills, MI, USA.

Antonio, C., Fausto, M., Andrea, T., and Giovanni, A. P. (2015). "Influence of polypropylene fibre reinforcement and width-to-effective depth ratio in wide-shallow beams." *Engineering Structures Journal*, Vol. 88, pp. 12-21, DOI: 10.1016/j.engstruct.2015.01.037.

Antonio, C., Fausto, M., and Giovanni, A. P. (2013). "Wide-shallow beams with and without steel fibres: A peculiar behaviour in shear and flexure." *Composite Part B Journal*, Vol. 51, pp. 282-290, DOI: 10.1016/j.compositesb.2013.03.033.

Antonio, C., Fausto, M., and Giovanni, A. P. (2017). "Influence of width-to-effective depth ratio on Shear strength of reinforced concrete elements without web reinforcement." *American Concrete Institute Structural Journal*, Vol. 114, No. 4, pp. 995-1006.

ASTM (2014a). *Standard test method for compressive strength of cylindrical concrete specimens*, ASTM C39-C39M-14, American Society for Testing and Materials (ASTM) International, West Conshohocken, PA, USA, DOI: 10.1520/C0039_C0039M-14.

ASTM (2014b). *Standard test method for static modulus of elasticity and Poisson's ratio of concrete in compression*, C469-C469M-14, American Society for Testing and Materials (ASTM) International, West Conshohocken, PA, USA, DOI: 10.1520/C0469_C0469M-14.

ASTM (2016). *Standard specification for deformed and plain carbon-steel bars for concrete reinforcement,* ASTM A615/A615M-16, American Society for Testing and Materials (ASTM) International, West Conshohocken, PA, USA, DOI: 10.1520/A0615_A0615M-16.

Bentz, E. C. (2005). "Empirical modeling of reinforced concrete shear strength size effect for members without stirrups." *American Concrete Institute Structural Journal*, Vol. 102, No. 2, pp. 232-241.

CSA (2004). *Design of concrete structures*, CAN/CSA A23.3-04, Canadian Standards Association, Mississauga, Ontario, Canada.

EN 1992-1-1 (2004). *Eurocode 2: Design of concrete structures - Part 1-1: General rules and rules for buildings*, European Committee for Standardization, Brussels, Belgium.

Kim, J. K. and Park, Y. D. (1996). "Prediction of shear strength of reinforced concrete beams without web reinforcement." *American Concrete Institute Material Journal*, Vol. 93, No. 3, pp. 213-222, DOI: org/10.1177/1369433217706778.

Lantsoght, O. L., Veen, D. C., Boer, E., and Walraven, J. C. (2015). "One-way slabs subjected to combination of loads failing in Shear." *American Concrete Institute Material Journal*, Vol. 112, No. 4, pp. 417-426, DOI: 10.14359/51687656.

Lubell, A. S., Bentz, E. C., and Collins, M. P. (2009a). "Shear reinforcement spacing in wide members." *American Concrete Institute Structural Journal*, Vol. 106, No. 2, pp. 205-214, DOI: 10.14359/56359.

Lubell, A. S., Bentz, E. C., and Collins, M. P. (2009b). "Influence of longitudinal reinforcement on one-way shear in slabs and wide beams." *Journal of Structural Engineering*, Vol. 135, No. 1, pp. 78-87, DOI: 10.1061/ (ASCE) 0733-9445(2009)135:1(78).

Mohammadyan, S. E., Marsono, A. K., Abdullah, R., and Moghadasi,

M. (2014). "Wide beam shear behavior with diverse types of reinforcement." *American Concrete Institute Structural Journal*, Vol. 111, No. 1, pp. 172-185, DOI: 10.14359/51687299.

Okamura, H. and Higai, T. (1980). "Proposed design equation for shear strength of RC beams without web reinforcement." *Japan Society of Civil Engineering*, Vol. 300, pp. 131-141, DOI: 10.2208/jscej1969.1980.300_131.

Rebeiz, K. S. (1999). "Shear strength prediction for concrete members." *Journal of Structure. Engineering*, Vol. 125, No. 3, pp. 301-308, DOI: 10.1061/(ASCE)0733-9445(1999)125:3(301).

Serna, R., Fernandez, P., Miguel, S., and Debb (2002). "Influence of stirrup distribution and support width on the shear strength of reinforced concrete wide beams." *Magazine of Concrete Research*, Vol. 54, No. 3, pp. 181-191, DOI: 10.1680/macr.2002.54.3.181.

Sherwood, E. G., Bentz, E. C., and Collins, M. P. (2007). "Effect of aggregate size on beam-shear strength of thick slabs." *American Concrete Institute Structural Journal*, Vol. 104, No. 2, pp. 180-190, DOI: 10.14359/51689720.

Sherwood, E. G., Lubell, A. S., Bentz, E. C., and Collins, M. P. (2006). "One-way shear strength of thick slabs and wide beams." *American Concrete Institute Structural Journal*, Vol. 103, No. 6, pp. 794-802, DOI: 10.14359/18229.

Zsutty, T. C. (1968). "Beam shear strength prediction by analysis of existing data." *American Concrete Institute Structural Journal*, Vol. 65, No. 111, pp. 943-951.